

Electromagnetically induced transparency in a V-system with ^{87}Rb vapor in the hyperfine Paschen–Back regime

CLARE. R. HIGGINS^{1,*} AND IFAN. G. HUGHES¹

¹Department of Physics, Durham University, South Road, Durham, DH1 3LE, UK

*Corresponding author: clare.r.higgins@durham.ac.uk

Compiled April 22, 2021

We observe EIT in a V-system in a thermal rubidium–87 vapor in the hyperfine Paschen–Back regime, realized with a 0.6 T axial magnetic field. In this regime energy levels are no longer degenerate and EIT features from different initial states are distinct. We compare our results to a model using the time-dependent Lindblad master equation, and having averaged over a distribution of interaction times, see good qualitative agreement for a range of pump Rabi frequencies. Excited state decay into both ground states is shown to play a prominent role in the generation of the transparency feature, which arises mainly due to transfer of population into the ground state not coupled by the probe beam. © 2021 Optical Society of America

<http://dx.doi.org/10.1364/ao.XX.XXXXXX>

Electromagnetically induced transparency (EIT) is an optical phenomenon involving three quantum states coupled by two optical fields (laser beams). In an absorbing medium, a transparency window in the transmission of a weak probe beam on one transition is induced by the presence of a strong pump beam on another transition. Throughout the text we refer to these beams as ‘pump’ and ‘probe’. EIT has been widely studied and has potential applications in precision magnetometers [1–3], quantum information [4, 5], and atomic clocks [6]. There are three possible configurations of EIT: V; lambda; and ladder [7]. V-EIT is the least studied of these because there is no stable dark state [8], as both of the singly coupled states are excited states and can decay to the ground state. Nevertheless, V-EIT has been extensively studied [9–20], and provides an interesting testing ground for ascertaining the relative importance of coherent and incoherent mechanisms in the generation of the transparency window [14, 21, 22].

One of the main obstacles to overcome in modelling and understanding V-EIT in thermal vapors is the complexity introduced by the overlapping spectral lines as a consequence of the degeneracies of the magnetic sub-levels and the excited-state hyperfine splitting being less than the Doppler width of the probed transition. To circumvent these difficulties, we use the hyperfine Paschen–Back regime [24–31] where the energy levels

are non-degenerate. A 0.6 T magnetic field used with ^{87}Rb on the D1 and D2 lines leads to isolated transitions separated by more than their Doppler width. Previous work has shown that operating in this regime allows simplified energy-level schemes and theoretical models, leading to good agreement between theory and experiment [32–35].

Our V-EIT system, realized in the hyperfine Paschen–Back regime, is shown in Fig. 1, part a). The driving Rabi frequencies are labelled Ω_{ab} , where a and b represent the initial and final states respectively. The decays between states have two contributions: the natural linewidth, Γ_{ab} , and a collisional decay to each ground state, γ . The second is present even where dipole-allowed transitions are forbidden, and the total collisional decay from an excited state has been experimentally determined in this cell as $2\gamma/2\pi = 7$ MHz. The levels we use, marked $|1\rangle$, $|2\rangle$ and $|3\rangle$ in the upper figure, do not form a closed system. We use ‘closed system’ to mean the atoms do not decay to any states outside of the three EIT levels, and ‘open system’ when decay to other, non laser-coupled states, is possible. The pumped transition – from $|1\rangle$ to $|3\rangle$ – is an open transition so $|3\rangle$ can decay to the other, uncoupled, ground state. This adds a fourth level into the system, which we label $|0\rangle$. The pump causes population transfer from $|1\rangle$ to $|0\rangle$, resulting in reduced absorption of the probe which couples $|1\rangle$ and $|2\rangle$. Part b) shows the state configuration when the probe is instead tuned to the transition between $|0\rangle$ and $|2\rangle$. This is not an EIT setup, but allows us to see the enhanced absorption caused by the extra population in $|0\rangle$.

We solve the Lindblad master equation [7] numerically for our four-level system. The pumping transition we use is open, as the excited state, $|3\rangle$, can decay to both m_j ground states, $|0\rangle$ and $|1\rangle$, as depicted in Fig. 1a). The pump and probe only couple to $|1\rangle$ so in the steady-state solution all the population ends up in the uncoupled ground state, $|0\rangle$, resulting in no absorption. We therefore have to use the time-dependent solutions. We have beams with $1/e^2$ radius of (97 ± 5) μm , from which we calculate the in-beam time-of-flight distribution, using the transverse velocity distribution [36–38]. For a given probe detuning the solutions are summed over all longitudinal velocity contributions [39]. The absorption profile is calculated from the imaginary part of the relevant coherence, and we use the Elecsus code [40] to calculate the linestrengths.

The experimental setup is shown in Fig. 2. We use a 2 mm

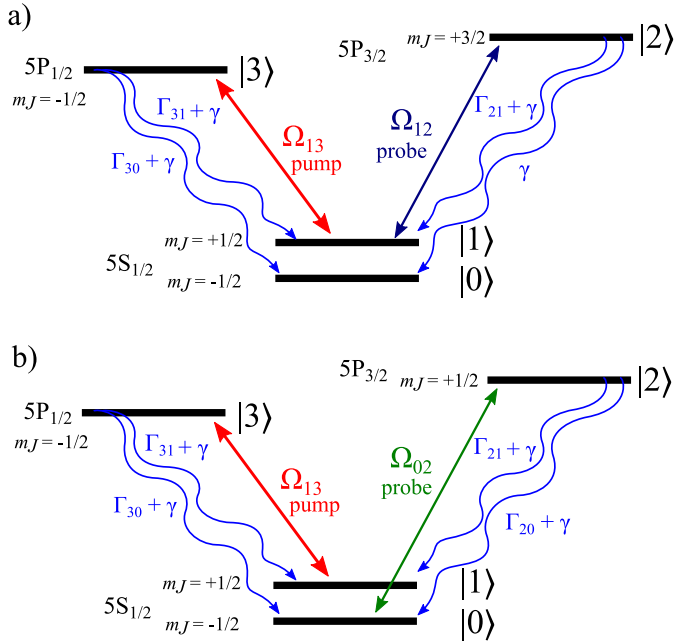


Fig. 1. The energy levels involved in our system. a) shows the EIT configuration, in which the 780 nm probe beam is coupling $m_J = +1/2$ to $m_J = +3/2$. In b) the probe beam is instead tuned to couple the $m_J = -1/2$ to $m_J = +1/2$ transition, which excites out of $|0\rangle$, the non-pump-coupled ground state. This configuration does not produce EIT, but demonstrates that population moves from $|1\rangle$ to $|0\rangle$. These two probe positions produce the set 1 and set 2 of peaks in Fig 3, respectively. The probe(pump) is left(right)-hand circularly polarized and couples $\sigma_+(\sigma_-)$ transitions [23].

long 98% ^{87}Rb vapor cell in a magnetic field, parallel to the laser propagation direction, of 0.6 T, produced by two cylindrical ‘top hat’ magnets. The orthogonally linearly polarized 795 nm and 780 nm beams are combined on a polarizing beam splitter. A quarter waveplate transforms the polarization to left-hand circular and right-hand circular respectively. A lens of focal length 200 mm focusses the beams to a waist of $(97 \pm 5) \mu\text{m}$ inside the cell. After the cell an interference filter removes pump light, and the probe transmission spectrum is measured on a photodiode. We have a strong, resonant 795 nm pump, and a weak 780 nm scanning probe. We use a vapor temperature of 80 °C; at lower temperatures the signals are smaller, and at higher temperatures the absorption saturates and the features are distorted.

The black trace in Fig 3 a) shows a scan of the 780 nm probe over the D2 absorption lines at 0.6 T, with no pump. Here, and throughout, we use a probe power of $0.3 \mu\text{W}$. All the optical power values reported throughout this work are measured before the vapor cell, and have an error of $\pm 5\%$. At 0.6 T, m_I and m_J are good quantum numbers. For ^{87}Rb , $I = 3/2$, therefore there are four possible values for m_I . The spectrum shows two sets of four transitions; in set 1(set 2) all four transitions are between states with initial $m_J = +1/2(-1/2)$ and final $m_J = +3/2(+1/2)$. Inside each set, each transition has a different m_I value, as labelled in the figure. The four colored traces show the probe transmission when the pump is tuned to the correspondingly colored transition in b). It is evident that when the pump is coupled to a particular m_I level in the upper ground

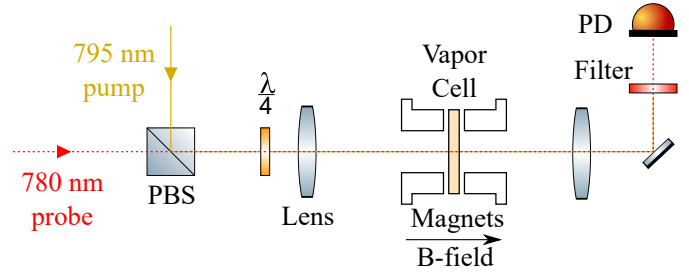


Fig. 2. Experimental setup. Orthogonally linearly polarized 795 nm pump and 780 nm probe beams are combined on a polarizing beam splitter (PBS) cube, and passed through a quarter waveplate converting them to right- and left-handed circularly polarized light, respectively. The beams are focussed through a 2 mm vapor cell in a longitudinal 0.6 T magnetic field, to a beam waist of $(97 \pm 5) \mu\text{m}$. The light transmitted through the cell passes through an interference filter to remove pump light, and is recorded on a photodiode (PD).

state, $|1\rangle$, there is a transmission window in the probe absorption peak coupling out of that level (set 1 transitions). There is also a corresponding enhanced-absorption feature when the probe instead couples out of the lower ground state with the same m_I value, $|0\rangle$ (set 2 transitions).

Fig 4 shows the effect of changing pump power/Rabi frequency on the transmission and absorption features, with experimental results in the upper panels and model predictions in the lower panels. Optical power is related to Rabi frequency by the area of the beam and the dipole matrix element of the transition. Here, as we are not plotting theory and experiment on the same axis we use optical power for experiment, and Rabi frequency for theory. We see good qualitative agreement, with both the narrow transmission and the extra absorption feature correctly predicted. The features are slightly narrower in theory than in experiment. In our model we assume that the beams have uniform intensity, whereas in reality they have a Gaussian profile; consequently atoms will experience a varying pump intensity as they traverse the beam. A more detailed numerical model beyond the scope of this work is required to fully account for the width of the EIT features.

Fig 5 shows the effect of changing pump detuning whilst keeping pump power constant at $20 \mu\text{W}$, and scanning the probe. Top panels show experimental results and bottom panels show model prediction. Changing the pump detuning selects atoms with a different longitudinal velocity, and concomitantly changes the frequency of the transmission (left) and enhanced absorption (right) features in the probe scan. This behaviour is predicted by the model, as shown in the lower two panels.

A relevant question in three-level-systems is whether the spectral features are caused by coherent or incoherent effects [8, 14]. The presence of a prominent coherent enhanced absorption feature on the transition out of the non-pump-coupled ground state, $|0\rangle$, is evidence that a significant part of the transmission feature does not arise from a coherent EIT effect, but instead from population transfer to a different (and uncoupled) ground state via velocity-selective optical pumping. However, the coherent process is still present, and we can use the model to see this. The density matrix element ρ_{23} is the coherence between $|2\rangle$ and $|3\rangle$, the excited states of our system. Fig. 6 compares the transmission (lower panel) and corresponding coherence (upper) for a closed system – meaning no decays into $|0\rangle$ – (dotted lines) and our

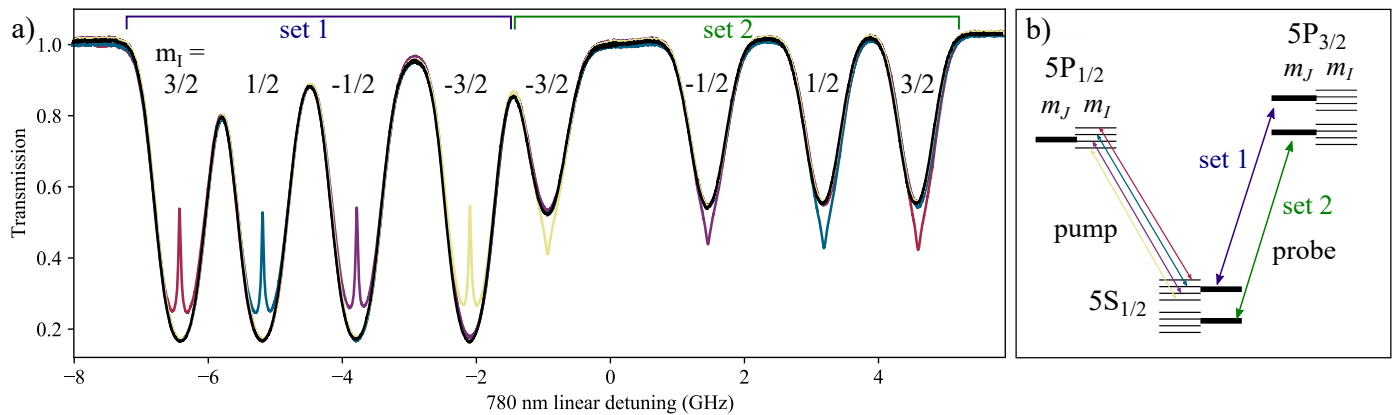


Fig. 3. a) shows a $0.3 \mu\text{W}$, 780 nm probe beam scan over the D2 transition lines at 0.6 T . The black trace is probe only, while the four colored traces show the effect of introducing a $20 \mu\text{W}$ pump beam on the correspondingly colored transition shown in b). Each of the four pump transitions has a different m_I value. Introducing a particular m_I pump transition induces a transparency in the peak in set 1, and an enhanced absorption feature in the corresponding peak in set 2, which have the same m_I .

open system (solid lines). A range of pump powers are plotted and colored according to the legend. We see that as pump power increases, the difference between the coherences in the closed and open systems increases. We also note that for a particular pump power the closed system coherence is greater than the open system coherence, while the open system transmission is greater than closed system transmission. This shows that in our open system the coherence is a small, but present, cause of the feature and that as the pump power increases, its proportional contribution decreases.

In conclusion, we have observed EIT in a V-system and the concomitant enhanced absorption. The importance of the allowed decay from the excited states to both ground states was emphasized. Our theoretical model captures all of the relevant processes, and gives insight into the role of coherence in explaining the observed narrow spectral features. The theoretical treatment is greatly simplified because the experiment was conducted in the hyperfine Paschen-Back regime, leading to distinct non-overlapping resonances.

Funding. EPSRC (EP/R002061/1); Durham University.

Acknowledgements. The authors thank Daniel Whiting for help with the model code, and Renju Mathew, Danielle Pizzey, Lina Marieth Hoyos-Campo and Tom Cutler for helpful discussions. The data presented in this paper are available from DRO, <https://doi.org/10.15128/r2t148fh16h>.

Disclosures. The authors declare no conflicts of interest.

REFERENCES

- M. Fleischhauer, A. B. Matsko, and M. O. Scully, *Phys. Rev. A* **62**, 013808 (2000).
- D. Budker and M. Romalis, *Nat. Phys.* **3**, 227 (2007).
- V. I. Yudin, A. V. Taichenachev, Y. O. Dudin, V. L. Velichansky, A. S. Zibrov, and S. A. Zibrov, *Phys. Rev. A* **82**, 033807 (2010).
- R. G. Beausoleil, W. J. Munro, D. A. Rodrigues, and T. P. Spiller, *J. Mod. Opt.* **51**, 2441 (2004).
- K. Hammerer, A. S. Sørensen, and E. S. Polzik, *Rev. Mod. Phys.* **82**, 1041 (2010).
- R. Santra, E. Arimondo, T. Ido, C. H. Greene, and J. Ye, *Phys. Rev. Lett.* **94**, 173002 (2005).
- M. Fleischhauer, A. Imamoglu, and J. P. Marangos, *Rev. Mod. Phys.* **77**, 633 (2005).
- S. Khan, V. Bharti, and V. Natarajan, *Phys. Lett. A* **380**, 4100 (2016).
- S. Dey, S. Mitra, P. Ghosh, and B. Ray, *Optik* **126**, 2711 (2015).
- R. Hazra and M. M. Hossain, *J. Phys. B: At. Mol. Opt. Phys.* **53**, 235401 (2020).
- A. Das, B. C. Das, D. Bhattacharyya, S. Chakrabarti, and S. De, *J. Phys. B: At. Mol. Opt. Phys.* **51**, 175502 (2018).
- Y. Hoshina, N. Hayashi, K. Tsubota, I. Yoshida, K. Shijo, R. Sugazono, and M. Mitsunaga, *J. Opt. Soc. Am. B* **31**, 1808 (2014).
- J. R. Boon, E. Zekou, D. J. Fulton, and M. H. Dunn, *Phys. Rev. A* **57**, 1323 (1998).
- A. Lazoudis, T. Kirova, E. H. Ahmed, P. Qi, J. Huennekens, and A. M. Lyyra, *Phys. Rev. A* **83**, 063419 (2011).
- J. R. Boon, E. Zekou, D. McGloin, and M. H. Dunn, *Phys. Rev. A* **59**, 4675 (1999).
- C. Zhu, C. Tan, and G. Huang, *Phys. Rev. A* **87**, 043813 (2013).
- D. McGloin, *J. Phys. B: At. Mol. Opt. Phys.* **36**, 2861 (2003).
- Y. Wu and X. Yang, *Phys. Rev. A* **71**, 053806 (2005).
- J. Zhao, L. Wang, L. Xiao, Y. Zhao, W. Yin, and S. Jia, *Opt. Commun.* **206**, 341 (2002).
- S. Scotto, D. Ciampini, C. Rizzo, and E. Arimondo, *Phys. Rev. A* **92**, 063810 (2015).
- H.-J. Kang and H.-R. Noh, *Opt. Express* **25**, 21762 (2017).
- D. J. Fulton, S. Shepherd, R. R. Moseley, B. D. Sinclair, and M. H. Dunn, *Phys. Rev. A* **52**, 2302 (1995).
- C. S. Adams and I. G. Hughes, *Optics f2f - From Fourier to Fresnel* (Oxford University Press, Oxford, UK, 2019).
- B. A. Olsen, B. Patton, Y.-Y. Jau, and W. Happer, *Phys. Rev. A* **84**, 063410 (2011).
- L. Weller, K. S. Kleinbach, M. A. Zentile, S. Knappe, C. S. Adams, and I. G. Hughes, *J. Phys. B: At. Mol. Opt. Phys.* **45**, 215005 (2012).
- M. A. Zentile, R. Andrews, L. Weller, S. Knappe, C. S. Adams, and I. G. Hughes, *J. Phys. B: At. Mol. Opt. Phys.* **47**, 075005 (2014).
- F. S. Ponciano-Ojeda, F. D. Logue, and I. G. Hughes, *J. Phys. B: At. Mol. Opt. Phys.* **54**, 015401 (2020).
- A. Sargsyan, G. Hakhumyan, C. Leroy, Y. Pashayan-Leroy, A. Papoyan, D. Sarkisyan, and M. Auzinsh, *J. Opt. Soc. Am. B* **31**, 1046 (2014).
- A. Sargsyan, E. Klinger, G. Hakhumyan, A. Tonoyan, A. Papoyan,

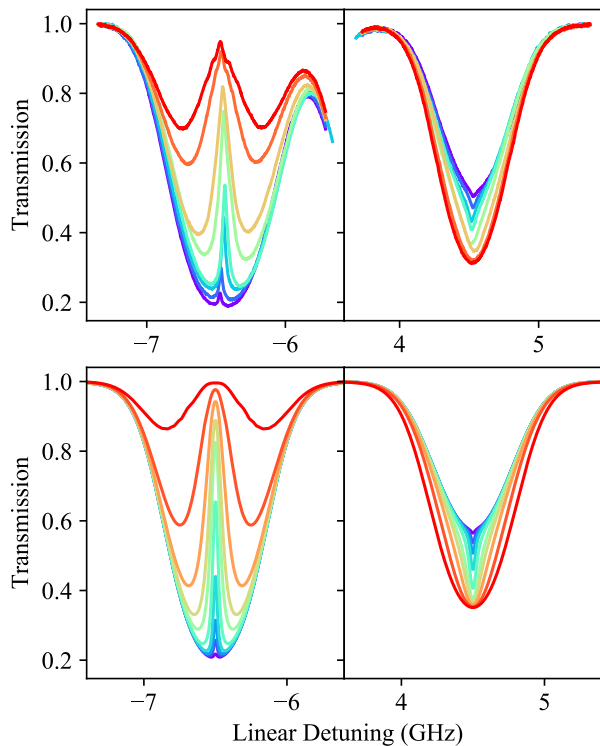


Fig. 4. The effect of changing the 795 nm pump power on the induced transparency and enhanced absorption features on the $m_l = +3/2$ transitions of the D2 (780 nm) spectrum. Upper: Experimental transmission spectra with changing pump powers, with values of in μW of 1 (purple), 5, 10, 20, 50, 100, 500, 1000 (red). These correspond to Rabi frequencies in the range 7 MHz–200 MHz. Lower: Modelled transmission spectra with pump Rabi frequencies in MHz of 1 (purple), 2, 3, 5, 10, 20, 30, 50, 100, 300 (red). The range of Rabi frequencies was chosen to straddle the range of features seen in the experimental data; the line colors are not calculated equivalents.

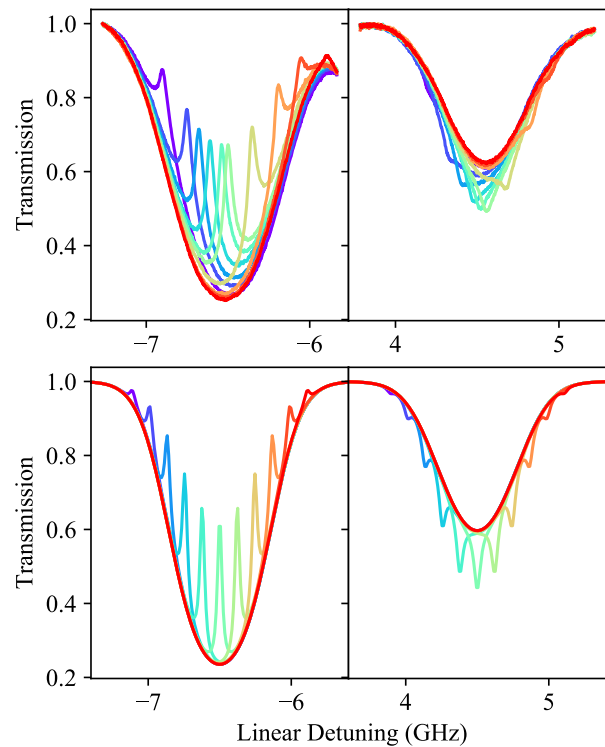


Fig. 5. The effect of changing the pump field detuning on the probe transmission and enhanced absorption features, for $m_l = +3/2$ transitions. The top two panels show experimental results, with a pump power of 20 μW . Bottom panels show the model prediction, using a pump Rabi frequency of 18 MHz. Blue to red traces are increasing pump frequency.

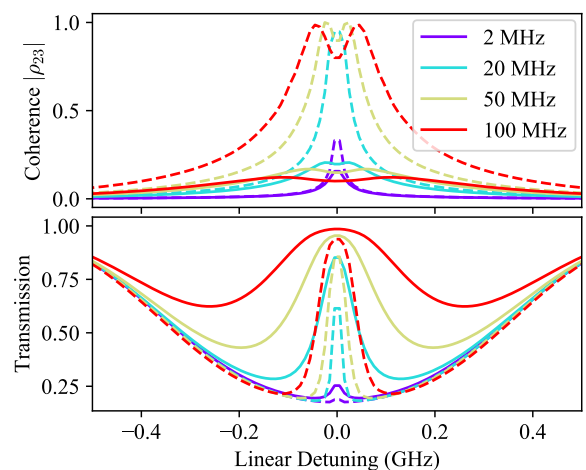


Fig. 6. Theoretical plot showing the coherence between excited states, and the corresponding probe transmission. On each plot we compare a closed system (dashed lines), and the open system of our experiment (solid lines), for linear pump Rabi frequencies as shown in the legend.

- C. Leroy, and D. Sarkisyan, *J. Opt. Soc. Am. B* **34**, 776 (2017).
30. L. Ma, D. A. Anderson, and G. Raithel, *Phys. Rev. A* **95**, 061804 (2017).
31. S. George, N. Bruyant, J. Béard, S. Scotto, E. Arimondo, R. Battesti, D. Ciampini, and C. Rizzo, *Rev. Sci. Instruments* **88**, 073102 (2017).
32. D. J. Whiting, J. Keaveney, C. S. Adams, and I. G. Hughes, *Phys. Rev. A* **93**, 043854 (2016).
33. D. J. Whiting, E. Bimbard, J. Keaveney, M. A. Zentile, C. S. Adams, and I. G. Hughes, *Opt. Lett.* **40**, 4289 (2015).
34. D. J. Whiting, R. S. Mathew, J. Keaveney, C. S. Adams, and I. G. Hughes, *J. Mod. Opt.* **65**, 713 (2018).
35. D. J. Whiting, N. Šibalić, J. Keaveney, C. S. Adams, and I. G. Hughes, *Phys. Rev. Lett.* **118**, 253601 (2017).
36. M. L. Harris, C. S. Adams, S. L. Cornish, I. C. McLeod, E. Tarleton, and I. G. Hughes, *Phys. Rev. A* **73**, 062509 (2006).
37. S. Ro Shin and H.-R. Noh, *J. Phys. Soc. Jpn.* **78**, 084302 (2009).
38. J. Sagle, R. K. Namiotka, and J. Huennekens, *J. Phys. B: At. Mol. Opt. Phys.* **29**, 2629 (1996).
39. I. G. Hughes, *J. Mod. Opt.* **65**, 640 (2018).
40. M. A. Zentile, J. Keaveney, L. Weller, D. J. Whiting, C. S. Adams, and I. G. Hughes, *Comput. Phys. Commun.* **189**, 162 (2015).

FULL REFERENCES

1. M. Fleischhauer, A. B. Matsko, and M. O. Scully, "Quantum limit of optical magnetometry in the presence of ac Stark shifts," *Phys. Rev. A* **62**, 013808 (2000).
2. D. Budker and M. Romalis, "Optical magnetometry," *Nat. Phys.* **3**, 227–234 (2007).
3. V. I. Yudin, A. V. Taichenachev, Y. O. Dudin, V. L. Velichansky, A. S. Zibrov, and S. A. Zibrov, "Vector magnetometry based on electromagnetically induced transparency in linearly polarized light," *Phys. Rev. A* **82**, 033807 (2010).
4. R. G. Beausoleil, W. J. Munro, D. A. Rodrigues, and T. P. Spiller, "Applications of electromagnetically induced transparency to quantum information processing," *J. Mod. Opt.* **51**, 2441–2448 (2004).
5. K. Hammerer, A. S. Sørensen, and E. S. Polzik, "Quantum interface between light and atomic ensembles," *Rev. Mod. Phys.* **82**, 1041–1093 (2010).
6. R. Santra, E. Arimondo, T. Ido, C. H. Greene, and J. Ye, "High-accuracy optical clock via three-level coherence in neutral bosonic ^{88}Sr ," *Phys. Rev. Lett.* **94**, 173002 (2005).
7. M. Fleischhauer, A. Imamoglu, and J. P. Marangos, "Electromagnetically induced transparency: Optics in coherent media," *Rev. Mod. Phys.* **77**, 633–673 (2005).
8. S. Khan, V. Bharti, and V. Natarajan, "Role of dressed-state interference in electromagnetically induced transparency," *Phys. Lett. A* **380**, 4100–4104 (2016).
9. S. Dey, S. Mitra, P. Ghosh, and B. Ray, "EIT line shape in an open and partially closed multilevel V-type system," *Optik* **126**, 2711–2717 (2015).
10. R. Hazra and M. M. Hossain, "Study of multi-window electromagnetically induced transparency (EIT) and related dispersive signals in V-type systems in the Zeeman sublevels of hyperfine states of 87Rb-D2 line," *J. Phys. B: At. Mol. Opt. Phys.* **53**, 235401 (2020).
11. A. Das, B. C. Das, D. Bhattacharyya, S. Chakrabarti, and S. De, "Polarization rotation with electromagnetically induced transparency in a V-type configuration of Rb D1 and D2 transitions," *J. Phys. B: At. Mol. Opt. Phys.* **51**, 175502 (2018).
12. Y. Hoshina, N. Hayashi, K. Tsubota, I. Yoshida, K. Shijo, R. Sugizono, and M. Mitsunaga, "Electromagnetically induced transparency in a V-type multilevel system of Na vapor," *J. Opt. Soc. Am. B* **31**, 1808–1813 (2014).
13. J. R. Boon, E. Zekou, D. J. Fulton, and M. H. Dunn, "Experimental observation of a coherently induced transparency on a blue probe in a Doppler-broadened mismatched V-type system," *Phys. Rev. A* **57**, 1323–1328 (1998).
14. A. Lazoudis, T. Kirova, E. H. Ahmed, P. Qi, J. Huennekens, and A. M. Lyyra, "Electromagnetically induced transparency in an open V-type molecular system," *Phys. Rev. A* **83**, 063419 (2011).
15. J. R. Boon, E. Zekou, D. McGloin, and M. H. Dunn, "Comparison of wavelength dependence in cascade-, Λ -, and Vee-type schemes for electromagnetically induced transparency," *Phys. Rev. A* **59**, 4675–4684 (1999).
16. C. Zhu, C. Tan, and G. Huang, "Crossover from electromagnetically induced transparency to Autler-Townes splitting in open V-type molecular systems," *Phys. Rev. A* **87**, 043813 (2013).
17. D. McGloin, "Coherent effects in a driven Vee scheme," *J. Phys. B: At. Mol. Opt. Phys.* **36**, 2861–2871 (2003).
18. Y. Wu and X. Yang, "Electromagnetically induced transparency in v -, Λ -, and cascade-type schemes beyond steady-state analysis," *Phys. Rev. A* **71**, 053806 (2005).
19. J. Zhao, L. Wang, L. Xiao, Y. Zhao, W. Yin, and S. Jia, "Experimental measurement of absorption and dispersion in V-type cesium atom," *Opt. Commun.* **206**, 341–345 (2002).
20. S. Scotto, D. Ciampini, C. Rizzo, and E. Arimondo, "Four-level N-scheme crossover resonances in Rb saturation spectroscopy in magnetic fields," *Phys. Rev. A* **92**, 063810 (2015).
21. H.-J. Kang and H.-R. Noh, "Coherence effects in electromagnetically induced transparency in V-type systems of 87Rb ," *Opt. Express* **25**, 21762–21774 (2017).
22. D. J. Fulton, S. Shepherd, R. R. Moseley, B. D. Sinclair, and M. H. Dunn, "Continuous-wave electromagnetically induced transparency: A comparison of V, Λ , and cascade systems," *Phys. Rev. A* **52**, 2302–2311 (1995).
23. C. S. Adams and I. G. Hughes, *Optics f2f - From Fourier to Fresnel* (Oxford University Press, Oxford, UK, 2019).
24. B. A. Olsen, B. Patton, Y.-Y. Jau, and W. Happer, "Optical pumping and spectroscopy of Cs vapor at high magnetic field," *Phys. Rev. A* **84**, 063410 (2011).
25. L. Weller, K. S. Kleinbach, M. A. Zentile, S. Knappe, C. S. Adams, and I. G. Hughes, "Absolute absorption and dispersion of a rubidium vapour in the hyperfine Paschen-Back regime," *J. Phys. B: At. Mol. Opt. Phys.* **45**, 215005 (2012).
26. M. A. Zentile, R. Andrews, L. Weller, S. Knappe, C. S. Adams, and I. G. Hughes, "The hyperfine Paschen-Back Faraday effect," *J. Phys. B: At. Mol. Opt. Phys.* **47**, 075005 (2014).
27. F. S. Ponciano-Ojeda, F. D. Logue, and I. G. Hughes, "Absorption spectroscopy and Stokes polarimetry in a 87Rb vapour in the Voigt geometry with a 1.5 T external magnetic field," *J. Phys. B: At. Mol. Opt. Phys.* **54**, 015401 (2020).
28. A. Sargsyan, G. Hakhumyan, C. Leroy, Y. Pashayan-Leroy, A. Papoyan, D. Sarkisyan, and M. Auzinsh, "Hyperfine Paschen-Back regime in alkali metal atoms: consistency of two theoretical considerations and experiment," *J. Opt. Soc. Am. B* **31**, 1046–1053 (2014).
29. A. Sargsyan, E. Klinger, G. Hakhumyan, A. Tonoyan, A. Papoyan, C. Leroy, and D. Sarkisyan, "Decoupling of hyperfine structure of Cs D1 line in strong magnetic field studied by selective reflection from a nanocell," *J. Opt. Soc. Am. B* **34**, 776–784 (2017).
30. L. Ma, D. A. Anderson, and G. Raithel, "Paschen-Back effects and Rydberg-state diamagnetism in vapor-cell electromagnetically induced transparency," *Phys. Rev. A* **95**, 061804 (2017).
31. S. George, N. Bruyant, J. Béard, S. Scotto, E. Arimondo, R. Battesti, D. Ciampini, and C. Rizzo, "Pulsed high magnetic field measurement with a rubidium vapor sensor," *Rev. Sci. Instruments* **88**, 073102 (2017).
32. D. J. Whiting, J. Keaveney, C. S. Adams, and I. G. Hughes, "Direct measurement of excited-state dipole matrix elements using electromagnetically induced transparency in the hyperfine Paschen-Back regime," *Phys. Rev. A* **93**, 043854 (2016).
33. D. J. Whiting, E. Bimbard, J. Keaveney, M. A. Zentile, C. S. Adams, and I. G. Hughes, "Electromagnetically induced absorption in a nondegenerate three-level ladder system," *Opt. Lett.* **40**, 4289–4292 (2015).
34. D. J. Whiting, R. S. Mathew, J. Keaveney, C. S. Adams, and I. G. Hughes, "Four-wave mixing in a non-degenerate four-level diamond configuration in the hyperfine Paschen-Back regime," *J. Mod. Opt.* **65**, 713–722 (2018).
35. D. J. Whiting, N. Šibalić, J. Keaveney, C. S. Adams, and I. G. Hughes, "Single-photon interference due to motion in an atomic collective excitation," *Phys. Rev. Lett.* **118**, 253601 (2017).
36. M. L. Harris, C. S. Adams, S. L. Cornish, I. C. McLeod, E. Tarleton, and I. G. Hughes, "Polarization spectroscopy in rubidium and cesium," *Phys. Rev. A* **73**, 062509 (2006).
37. S. Ro Shin and H.-R. Noh, "Calculation and measurement of absolute transmission in rubidium," *J. Phys. Soc. Jpn.* **78**, 084302 (2009).
38. J. Sagle, R. K. Namiotka, and J. Huennekens, "Measurement and modelling of intensity dependent absorption and transit relaxation on the cesium line," *J. Phys. B: At. Mol. Opt. Phys.* **29**, 2629–2643 (1996).
39. I. G. Hughes, "Velocity selection in a Doppler-broadened ensemble of atoms interacting with a monochromatic laser beam," *J. Mod. Opt.* **65**, 640–647 (2018).
40. M. A. Zentile, J. Keaveney, L. Weller, D. J. Whiting, C. S. Adams, and I. G. Hughes, "ElecSus: A program to calculate the electric susceptibility of an atomic ensemble," *Comput. Phys. Commun.* **189**, 162–174 (2015).